JOURNAL OF Applied Polymer SCIENCE

Flame Retardance and Origin of Bismaleimide Resin Composites with Green and Efficient Aluminum Phosphates

Qiuqin You, Li Yuan, Hong Wang, Guozheng Liang, Aijuan Gu

Department of Materials Science and Engineering, Jiangsu Key Laboratory of Advanced Functional Polymer Design and Application, College of Chemistry, Chemical Engineering and Materials Science, Soochow University, Suzhou, Jiangsu 215123, China

Correspondence to: A. Gu (E-mail: ajgu@suda.edu.cn) and G. Liang (E-mail: lgzheng@suda.edu.cn)

ABSTRACT: Developing green and high efficiency inorganic flame retardants is the trend of preparing flame retarding polymer composites. Aluminum phosphates (t-hAP) with uniform, small dimension, and hexagonal structure were facilely synthesized, which have similar size (1–2 μm) but different structures from commercial spherical-like aluminum phosphate (cAP). The flame retardance of bismaleimide (BD)/t-hAP and BD/cAP composites were intensively investigated. t-hAP is proved to have much better flame retarding effect than cAP, but also exhibits advantages over $Mg(OH)_2$ and $Al(OH)_3$. With only 5 wt % addition of t-hAP into BD resin, the peak and total heat releases as well as total smoke production significantly reduce 42.3, 47.8, and 67.3%, respectively; besides, better data are obtained as the loading of t-hAP increases to 10 wt %. These attractive data result from three effects induced by t-hAP. Besides the better protection role of sheet structure, the strong hydrogen bonding between t-hAP and BD resin endows the composite with good dispersion of t-hAP and high crosslinking density; moreover, t-hAP releases H_2O and NH_3, diluting flammable gases during combustion. © 2014 Wiley Periodicals, Inc. J. Appl. Polym. Sci. **2014**, *131*, 41089.

KEYWORDS: composites; flame retardance; thermosets

Received 19 March 2014; accepted 30 May 2014

DOI: 10.1002/app.41089

INTRODUCTION

High performance polymers with outstanding integrated properties have been increasingly required by the rapid development of cutting-edge fields such as electronic information, new energy, aerospace, insulation, and so on.[1,2] Flame retardance becomes one essential property besides good processing characteristics, high thermal, and mechanical properties.[3,4] However, almost all polymers are lack of flame retardance. Lots of researches have proved that the addition of flame retardants into a polymer is an easy and effective way to prepare flame retarding polymer composites.[5,6] Recently, inorganic flame retardants have attracted wide attentions because their low toxicity and noncorrosiveness meet the developing trend on green and efficiency for flame retardants.[7–9]

The main flame retarding process of available inorganic flame retardants such as $Mg(OH)_2$ and $Al(OH)_3$ is the decomposition of the compounds at a specific temperature with the elimination of water. This endothermic process removes energy from the system, while the evaporated water serves to dilute flammable pyrolysis gases at the same time.[10,11] However, to achieve acceptable combustion resistance, the concentration of inorganic flame retardants should be large enough (for example up to 50 wt % or even more),[12] but such high level of addition definitely in turn leads to deteriorated processing characteristics and mechanical property.[13,14] Hence, to find a high efficiency and environmentally friendly inorganic flame retardant while maintaining the outstanding performances of original polymer is still a challenge.

For a long time, tremendous growth has been taken place to overwhelm any new attempt in preparing new functional fillers; however, there is still plenty of opportunity for finding new functional fillers by looking at existed fillers in a modified form. Aluminum phosphate (AP) is an important inorganic filler that is famous for its outstanding chemical and thermal stability, thermal-shock, and thermal oxidation resistance; moreover, as APs show the features of both metal and ceramic at high temperature,[15–17] so AP can meet a variety of special requirements. In fact, AP has been used as the matrix of advanced wave-transparent composites,[18] or the coating for preparing composites with outstanding thermo oxidative stability.[19,20] Goedelt's group[21] found that the thermal oxidative stability of carbon fibers was greatly improved by depositing AP coating with a thickness of 25 nm. Huang's[22] and Deng's associates[23] pointed

out that silica/AP and organosilicon/AP composites had good thermal stability. Our group found that cyanate ester (CE)/AP composites have much higher char yield (Y_c) at high temperature than CE resin, and the experimental Y_c values of the composites are higher than the value calculated using the "mixture rule".[24]

Above researches have proved that AP has an obvious effect on improving the thermal stability of polymers, which provides a possibility for getting good flame retardance[25,26]; however, this is not an inevitable trend.[27] Considering the importance and wide application as well as the nontoxicity, it is interesting to evaluate the flame retarding ability of AP. On the other hand, as the members of the same family of AP, aluminum hypophosphite[28] and aluminum diethylphosphinate[29] have been reported to be flame retardants, but the flame retardance of polymer/AP composites has not been reported yet.

On the other hand, previous studies have shown that sheet-like materials, montmorillonite[30] and zirconium phosphate,[31] have outstanding thermal stability and flame retardance. Qu[32] synthesized a series of needle, plate, and rod-like $Mg(OH)_2$, and found that plate like $Mg(OH)_2$ had better flame retardance than others. Therefore, it is interesting to synthesize AP with plate like structure.

Bismaleimide (BMI) is the representative of heat-resistant thermosetting resins, and its unique integrated performances, including outstanding heat and moisture resistance, high strength, good process characteristics, and so on,[33] endowing BMI with great potential of applications in many cutting-edge fields. Therefore, BMI resin was studied as a valuable model to evaluate the possibility that AP acts as the flame retardant, and the influence of structure of AP on the flame retardance. Some interesting phenomena were observed, and the origin behind was studied.

EXPERIMENTAL

Materials

Phosphoric acid (H_3PO_4, 85 wt %) was bought from Sinopharm Chemical Reagent (China). $Al(OH)_3$ (chemical grade) was purchased from Jinan Jingyinghan Chemical (China). Cetyl trimethyl ammonium bromide (CTAB) was obtained from Sinopharm Chemical Reagent (China). Ammonia and ethanol with analytical grades were commercial products and used without further purification. BMI used herein was 4, 4′-bismaleimidophenyl methane (BDM), which was obtained from Northwestern Institute of Chemical Engineering (China). 2, 2′-Diallyl bisphenol A (DBA) was purchased from Laiyu Chemical Factory (China). Commercial AP (cAP) was brought from Meixing Chemical of Shanghai (China).

Synthesis of Hexagonal AP (hAP)

$Al(OH)_3$ and H_3PO_4 reacted at 80°C to get $Al(H_2PO_4)_3$, which acted as the precursor of following reactions. Ammonia (the precipitating agent) was gradually dropped in $Al(H_2PO_4)_3$ until the pH value of the solution reached 5 to produce hAP.

In detail, a total of 200 mL CTAB solution (0.01 mol/L) was added into a 500-mL three-necked flask at 80°C that contained $Al(H_2PO_4)_3$ with stirring. After staying for 10 min, adjusted the temperature to 60°C, and then, aqueous ammonia (28 wt %) was slowly dropped into the flask for 30 min. When the pH of the solution in the flask reached 5, it was the end of titration. After maintained at 60°C for 10–12 h, this suspension was filtered, washed with water and ethanol, successively, for six times to remove impurities, followed with drying at 80°C for 24 h. The resultant white powder was hAP.

hAP was thermally treated at 150°C for 2 h or 300°C for 2 h, and the resultant sample was coded as t-hAP or tt-hAP.

Preparation of BMI Resin

BDM and DBA with a molar ratio of 1 : 0.86 were blended at 135°C for 30 min with stirring to obtain a transparent liquid (prepolymer). The prepolymer was thoroughly degassed to remove entrapped air at 135°C in a vacuum oven. Subsequently, the mold was put into an oven for curing and postcuring following the protocol of 150°C/2 h+180°C/2 h+200°C/2 h and 230°C/4 h, successively, and the resultant resin was coded as BD.

Preparation of Composites

DBA and t-hAP were blended at 80°C with vigorous stirring and ultrasound for 30 min to form a uniform solution, into which BDM was added at 135°C for an additional 30 min to get BD/t-hAP prepolymer.

The prepolymer was thoroughly degassed to remove entrapped air at 135°C in a vacuum oven. Subsequently, the mixture was cast into a mold for curing and postcuring following the protocol of 150°C/2 h+180°C/2 h+200°C/2 h and 230°C/4 h, successively. Finally the composite was demolded and coded as BD/nt-hAP composite, where n represents the weight loading of t-hAP in BD/t-hAP system, taking the values of 5, 10, 15, and 20.

Using above procedure, BD/cAP composite was also prepared except that t-hAP was replaced by cAP.

Characterizations

Solid state ^{31}P NMR spectra were recorded on a Bruker AV-500 MHZ spectrometer with magic angle spinning (MAS) at 15 kHz. NMR shifts are given in δ with positive value downfield of external H_3PO_4 (^{31}P, δ 0) reference.

Fourier transform infrared (FTIR) spectra were recorded with a resolution of 2 cm^{-1} on a Prostar LC240 Infrared Spectrometer (USA) between 400 and 4000 cm^{-1}.

Thermogravimetric (TG) analyses were performed on a TGA SDTQ600 (TA Instruments, USA) in the range from 25 to 800°C in a nitrogen atmosphere at a heating rate of 10°C/min.

Powder X-ray diffraction (XRD) patterns were obtained on a MERCURY CCD X-Bray diffractometer (RIGAKu, Japan) with CuKα radiation. The 2θ angle ranged from 5 to 80°, and the scanning rate was 10°/min.

Dynamic mechanical analysis (DMA) scans were performed using TA DMA Q800 apparatus from TA Instruments (USA). A single cantilever clamping geometry was used. DMA tests were carried out from 100 to 350°C with a heating rate of 3°C/min at 1 Hz. The dimensions of each sample were $(35 \pm 0.02) \times (13 \pm 0.02) \times (3 \pm 0.02)$ mm^3.

$$Al(OH)_3 + 9H^+ + 3PO_4^{3-} \xrightarrow{80\,^oC} Al^{3+} + 3H_2PO_4^- + 3H_2O$$
$$H^+ + NH_3{\cdot}H_2O \xrightarrow{60\,^oC} NH_4^+ + H_2O$$
$$Al^{3+} + PO_4^{3-} \xrightarrow{60\,^oC} AlPO_4$$
$$5AlPO_4 + 3NH_4^+ + 3H_2PO_4^- \xrightarrow{60\,^oC} (NH_4)_3Al_5H_6(PO_4)_8\downarrow$$

Scheme 1. The synthesis mechanism of hAP.

Flammability of resins was characterized using a cone calorimeter performed in a FTT0007 device from Fire Testing Technology Limited (UK) according to ISO 5660 with an incident flux of 35 kW/m^2 using a cone shape heater. The dimensions of sample were (100 ± 0.02) mm × (100 ± 0.02) mm × (3 ± 0.02) mm. For each resin or composite, three specimens were tested. Typical results from cone calorimeter were reproducible to within about ±10%, and the data reported here were the averages of triplicate.

Thermogravimetric analysis infrared (TG-IR) spectra were recorded using a TGA F1 (Netzsch, Germany) thermogravimetric analyzer that was interfaced to a TENSOR 27 (Bruker, Germany) FTIR spectrophotometer. About 10.0 mg of the sample was put in an alumina crucible and heated from 30 to 800°C with a heating rate of 10°C/min under a nitrogen atmosphere, and the flowing rate was 20 mL/min.

RESULTS AND DISCUSSION

Synthesis and Characterization of hAP

As stated in the introduction part, one aim of our investigation reported herein is synthesizing plate-like AP. In addition, it is known that the good dispersion of inorganic fillers in the organic resin is the guarantee to get good integrated performances, so the synthesized hAP is expected to have interaction with BD resin. Briefly, the chemical and morphological structures are two important things to be addressed.

hAP was synthesized using the homogeneous precipitation method through the mechanism shown in Scheme 1.[34,35] To confirm the chemical composition, FTIR and XRD techniques were used. The FTIR spectrum of hAP is shown in Figure 1, which has characteristic peaks assigning to the O—P—O bending vibration (ca. 474 cm^{-1}), P—O stretching vibration of $(PO_4)^{3-}$ (ca. 714 cm^{-1}) and the stretching vibration of Al—O in combination with P—O (ca. 1120 cm^{-1}),[36] preliminarily reflecting that hAP is $AlPO_4$. Moreover, the spectrum also shows the bending mode of HOH (1630 cm−1) and characteristic peaks of NH_4^+ (3244, 1400 cm^{-1}), demonstrating that hAP prepared has H_2O and NH_4^+. Note that these bounded compounds will be released when hAP is heated to enough high temperatures (for example, >100°C), so the concentration of these compounds should not be very large, otherwise when hAP is blended with BD resin at the temperature higher than 100°C, a large amount of water and NH_3 will be released, and thus make it impossible to prepare composites with good quality. Therefore, the prepared hAP has to be thermally treated to reduce the content of these compounds.

To select the procedure of the thermal treatment, the TG and DTG curves of hAP in a N_2 atmosphere were recorded. As shown in Figure 2, there are two peaks in the DTG curve according to the temperature with the maximum decomposing rate (T_{max}), one is the strong peak that takes place over the range from 100 to 150°C, and the other is a very small peak that occurs from 200 to 300°C. Therefore, two procedures, 150°C for 2 h and 300°C for 2 h, were used to treat hAP, respectively.

Figure 1 also gives the FTIR spectra of the two treated hAPs. It can be seen that after treated at 150°C for 2 h, the resultant sample (t-hAP) still has the characteristic peaks of NH_4^+ and H_2O, but the intensities are greatly reduced. However, after heated at 300°C for 2 h, no characteristic peaks of NH_4^+ can be observed in the spectrum of the sample (coded as tt-hAP), similar as the spectrum of cAP. Considering the requirement of good flame retardance, treated hAP particles with some NH_4^+ and H_2O were selected as the inorganic fillers to prepare BD

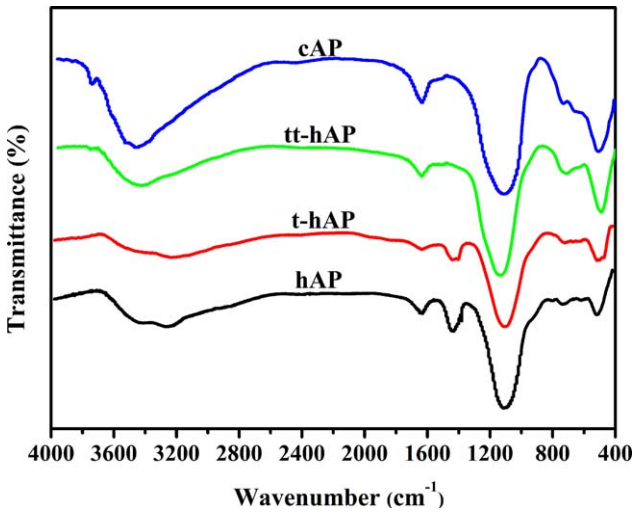

Figure 1. FTIR spectra of hAP, t-hAP, tt-hAP, and cAP. [Color figure can be viewed in the online issue, which is available at wileyonlinelibrary.com.]

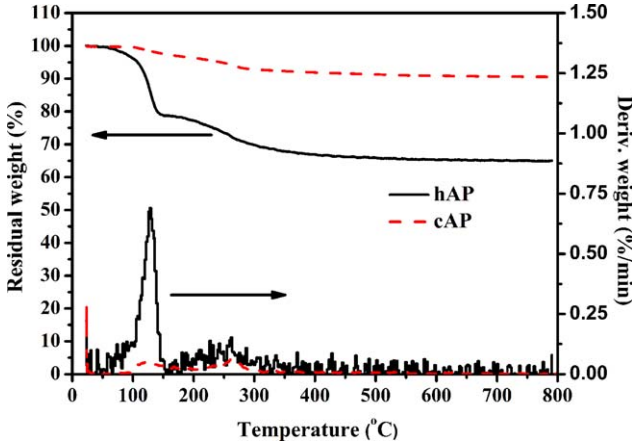

Figure 2. TG and DTG curves of *h*AP and cAP in a nitrogen atmosphere. [Color figure can be viewed in the online issue, which is available at wileyonlinelibrary.com.]

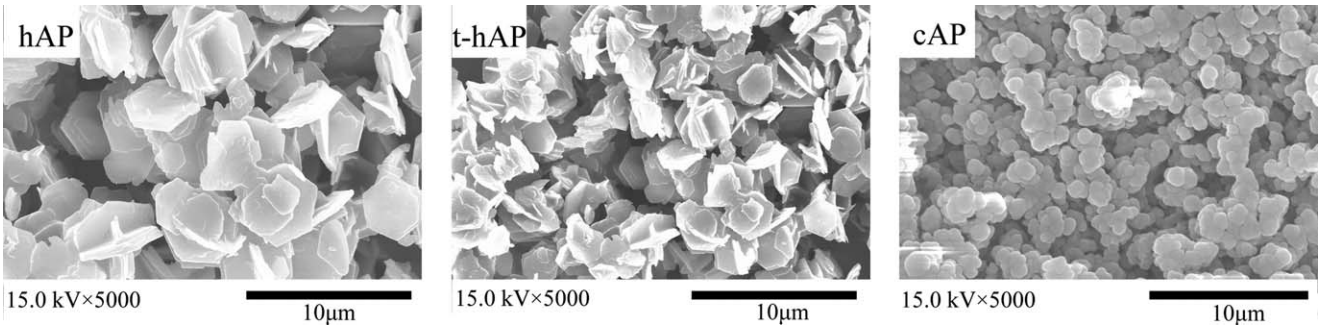

Figure 3. SEM images of hAP, t-hAP, and cAP.

resin composites. So the procedure for treating hAP is selected at 150°C/2 h.

Figure 3 shows the SEM images of cAP, hAP, and t-hAP. Different from the spherical like of cAP, either original or treated hAP exhibits a plate structure, meaning that the treatment does not change the hexagonal and plate-like morphology of hAP. The difference between hAP and t-hAP is their sizes, Specifically, the average sizes of hAP and t-hAP are about 2–3 and 1–2 μm, respectively, and the latter is similar as that of cAP.

Figure 4 shows the ^{31}P MAS NMR spectrum of hAP, which has two peaks at 5.7 and −18.5 ppm with an intensity ratio of 1 : 7, revealing that phosphate groups exist in two environments, one is protonated (5.7 ppm), and the other is nonprotonated (−18.5 ppm).[37] These results are in agreement with those of a natural taranakite sample.[38]

XRD is one of most important technique to characterize the structure of inorganic compounds.[39] Figure 5 gives the XRD patterns of hAP and t-hAP. A main diffraction peak of taranakite phase appears at 6° (2θ), suggesting that hAP belongs to ammonium analogue of the aluminum phosphate mineral taranakite (JSD 00-028-0041).[38] After treated at 150°C for 2 h, a significantly different pattern appears due to the loss of H_2O and NH_4^+. Specifically, the XRD pattern of t-hAP contains patterns of two aluminum phosphates, of which the dominated peaks well match the standard card PDF2 No. 47-0603 for $AlPO_4$-14 selected from the International Centre for Diffraction Data (ICDD) database; and minor peaks match well the standard card PDF2 No. 40-0404 for $Al_2(NH_4)(OH)(PO_4)_2{\cdot}2H_2O$ in the ICDD database,[40] so t-hAP has two crystal structures, and can be regarded as aluminum phosphates.

Flame Retardance of BD/t-hAP and BD/cAP Composites

Cone calorimeter test is an effective technique for simulating the real fire of materials in laboratory, from which many meaningful parameters will be obtained, such as ignition behavior, heat release, and smoke evolution.[41] BD/t-hAP composites could not be ignited under the irradiation flow at 35 kW/m^2; however, BD/cAP composites could, preliminarily suggesting that t-hAP has much better flame retarding effect than cAP. To make a quantitative comparison, the sparking manner was used to carry out cone calorimeter tests for both BD/t-hAP and BD/cAP composites.

Table I summarizes the typical data of BD resin, BD/cAP and BD/t-hAP composites from cone calorimeter tests. Each value has its own physical meaning, which represents the flame retardance from a specific angle; hence, the combination of these data will give us a full knowledge on the flame retardance of the materials.

Fire performance index (FPI), defined as the ratio of the time to ignition (TTI) to the peak of heat release rate (pHRR), has been suggested to be a parameter that relates to the time to

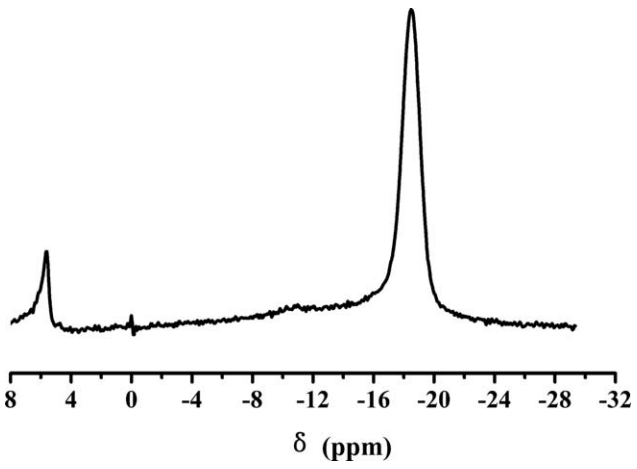

Figure 4. The ^{31} P MAS NMR spectrum of *h*AP.

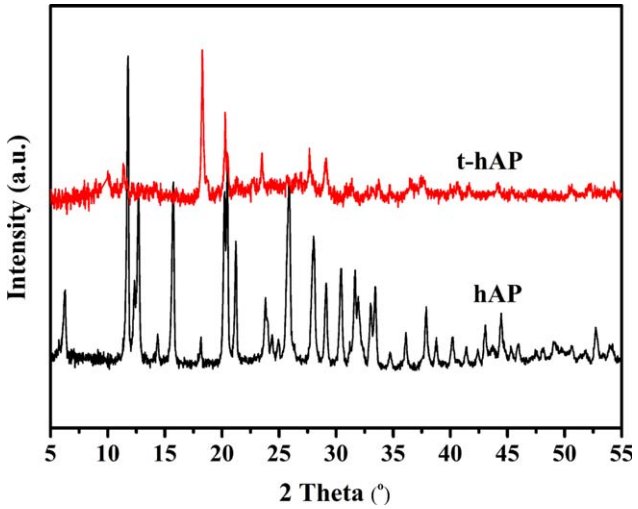

Figure 5. XRD patterns of original and treated hAPs. [Color figure can be viewed in the online issue, which is available at wileyonlinelibrary.com.]

Table I. Typical Data of BD Resin, BD/cAP, and BD/t-hAP Composites from Cone Calorimeter Tests

Sample	FPI (m^2s/kW)	TTI (s)	pHRR (kW/m^2)	THR (MJ/m^2)	Mean CO (kg/kg)	TSR (m^2)
BD	0.32 ± 0.01	108 ± 2	334.4 ± 20	76.28 ± 3.0	0.096 ± 0.005	21.46 ± 2
BD/5cAP	0.49 ± 0.01	117 ± 1	238.4 ± 18	58.33 ± 2.8	0.043 ± 0.002	14.27 ± 1
BD/10cAP	0.52 ± 0.01	121 ± 3	233.3 ± 16	49.64 ± 1.2	0.052 ± 0.003	13.46 ± 1
BD/15cAP	0.47 ± 0.01	120 ± 2	231.8 ± 20	46.14 ± 3.0	0.043 ± 0.002	9.46 ± 0.8
BD/20cAP	0.45 ± 0.01	120 ± 3	265.9 ± 25	56.81 ± 1.5	0.051 ± 0.002	12.39 ± 0.5
BD/5t-hAP	0.52 ± 0.01	101 ± 2	192.8 ± 12	39.85 ± 1.5	0.042 ± 0.001	7.02 ± 0.7
BD/10t-hAP	0.79 ± 0.01	112 ± 3	142.5 ± 15	39.23 ± 2.2	0.032 ± 0.003	7.31 ± 0.5
BD/15t-hAP	0.79 ± 0.02	102 ± 2	128.6 ± 14	32.56 ± 2.5	0.031 ± 0.001	5.72 ± 0.5
BD/20t-hAP	0.57 ± 0.01	94 ± 3	163.8 ± 17	37.51 ± 3.0	0.041 ± 0.002	6.75 ± 0.6

flash over in a full-scale fire situation, and thus refers to the risk of materials for catching fire.[42] All composites have higher FPI values than BD resin, demonstrating that the addition of either cAP or t-hAP into BD resin can effectively reduce the risk of the resin for catching fire. Noting that t-hAP shows remarkable advantage over cAP, for example, FPI values of BD/10t-hAP and BD/10cAP composites are 2.5 and 1.6 times of that of BD resin, respectively.

Heat release rate (HRR), including peak heat release rate (pHRR) and total heat release (THR), is the most important parameter that represents the intensity of combustion under the test condition.[43] Figure 6 shows the HRR as a function of time. BD resin has a broad and asymmetrical peak, which exhibits two peaks around the pHRR and lasts 144 s, indicating that the initially formed char is not strong enough to retard the continuous combustion. With the addition of 5 wt % cAP, a board HRR peak is found, but the intensity is reduced. As the content of cAP increases, the width and height of the HRR peak gradually become narrower and weaker. This trend also appears in the BD/t-hAP composites except that the change degree is much obvious. For example, the pHRR and THR values of BD/5cAP composite are about 71.2% and 74.6% of those of BD resin, respectively; while those of BD/5t-hAP composite are severally only 57.7% and 52.2% of those of BD resin.

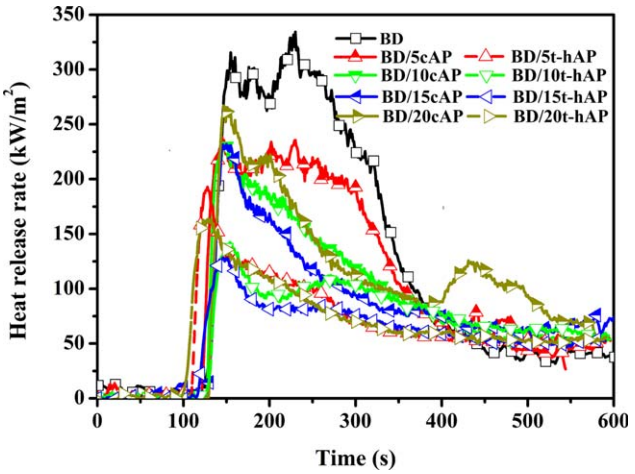

Figure 6. Overlay plots of dependence of HRR on time for BD resin, BD/cAP and BD/ t-hAP composites. [Color figure can be viewed in the online issue, which is available at wileyonlinelibrary.com.]

Previous studies found that zirconium phosphate,[44] carbon nanotube,[45] or clay[46] can only significantly reduce the pHRR value but not the THR. This phenomenon was also observed in the composites containing $Mg(OH)_2$ and $Al(OH)_3$. For example, with the addition of 40 wt % $Mg(OH)_2$ into high impact polystyrene, the pHRR was reduced 67.7%, but the THR was only reduced 9.2%.[47] Similarly, the addition of 47.5 wt % $Al(OH)_3$ into poly(ethylene-*co*-vinyl acetate) brings 71% reduction of pHRR and 25% reduction of THR.[48] Therefore, both t-hAP and cAP, especially t-hAP, have obvious advantage over these classic inorganic fillers in reducing HRR and THR.

The origin behind the different shapes of HRR-time plots for BD resin, BD/cAP and BD/t-hAP composites may be revealed through the discussion of the dependence of the normalized mass loss on the time during the whole combustion process as shown in Figure 7(a). After ignition, BD resin quickly loses its weight; while the two composites lose their weights in much slower rates, especially BD/t-hAP composites. For each kind of composites, with the increase of the content of fillers, the residual mass increases and reaches the maximum value and then decreases. The maximum values for BD/cAP and BD/t-hAP composites are 10 and 15 wt %, respectively. This is because the dispersion of fillers is closely related to the nature and the content of fillers. Generally, the presence of cAP and t-hAP can retard the mass loss, so the more loading tends to get big retarding effect; however, when the content of fillers is large enough, the agglomeration of fillers is obvious. As a result, the retarding effect of fillers is also dependent on the content of fillers. Note that BD/5t-hAP composite has higher residue than all BD/cAP composites, so t-hAP has much better flame retarding effect than cAP.

Figure 7(b) is the digital photos of residual chars for BD resin, BD/10cAP, and BD/10t-hAP composites after cone calorimeter tests. All chars have enlarged sizes than their original material, but BD/hAP char has the smallest enlarging degree, other two chars have similar enlarging degree. Besides this difference, the three chars have different morphologies. In detail, the surface of

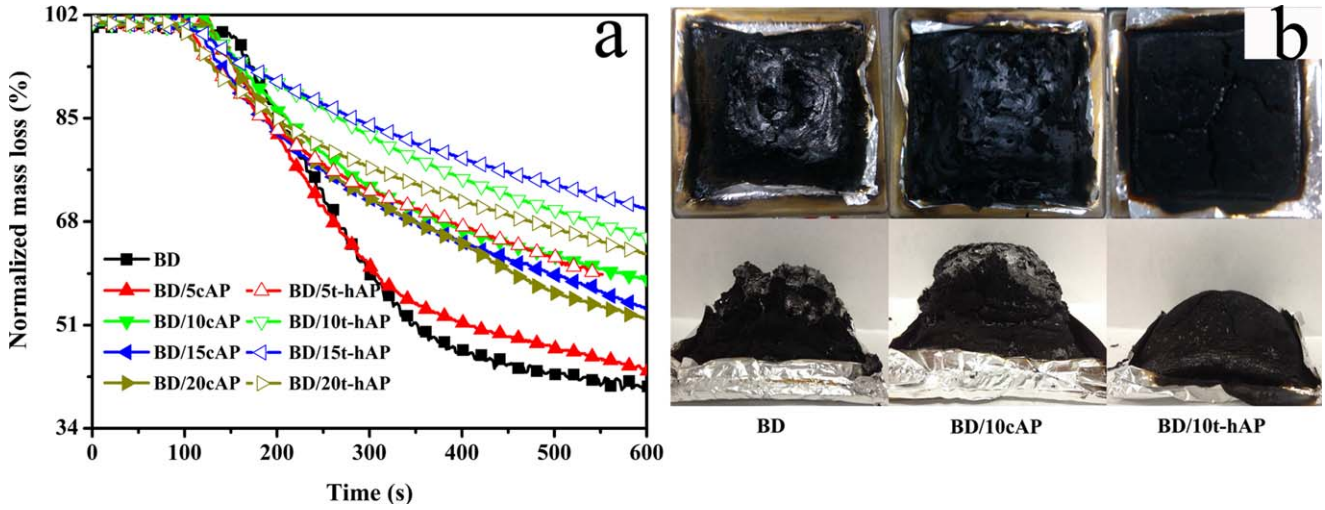

Figure 7. Overlay plots of dependence of mass on time (a) and digital photos of chars for BD resin, BD/10cAP and BD/10t-hAP composites (b). [Color figure can be viewed in the online issue, which is available at wileyonlinelibrary.com.]

BD char is so thin and loose that is easy to collapse. This phenomenon is somewhat changed by the addition of cAP, while the residue of BD/10t-hAP composite is completely different, its char is thick and compact. These phenomena indicate that the flame retarding effect of t-hAP is different from that of cAP. Detail discussion is presented in the following part.

As we've known that high smoke suppression becomes one important index of evaluating the flame retardance of a material because it is smoke, rather than the heat, that is responsible for the death in real fire hazards.[49] CO is the major toxic gas for halogen-free flame retardants.[50,51] The mean CO release of BD/t-hAP or BD/cAP composite is only 32–44% or 45–54% of that of BD resin. It was found that the addition of alkyl phosphinate,[52] clay,[53] or $Mg(OH)_2$[54] into polymers would increase the CO release. For example, the addition of $Mg(OH)_2$ to poly(vinyl chloride) would increase the average release of CO from 1.20 to 1.44 kg/kg.[54] Therefore, it is reasonable to state that t-hAP and cAP have attractive ability of reducing the generation of CO, and they are green flame retardants, especially t-hAP.

Figure 8 shows the overlay curves of smoke produce rate (SPR) as a function of time for BD resin, BD/cAP and BD/t-hAP composites. All BD/t-hAP composites have lower SPR values than BD/cAP composites, and the SPR values of BD/t-hAP and BD/cAP composites are only about 29–44% of that of BD resin, so does the total smoke production (TSP) values (Table I), hence both cAP and t-hAP have effective ability of smoke suppression, while the ability of t-hAP is much better. Magnesium hydroxides are famous for their high smoke suppression;[55] however, to achieve the same effect as t-hAP, their additions should be as high as 50 wt %.[56] Obviously, such high loading of magnesium hydroxides usually leads to poor processing characteristic and mechanical performances.

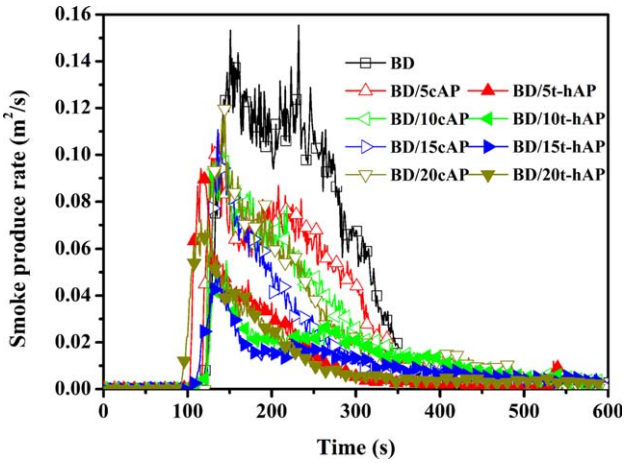

Figure 8. Overlay plots of dependence of SPR on time for BD resin, BD/cAP, and BD/t-hAP composites. [Color figure can be viewed in the online issue, which is available at wileyonlinelibrary.com.]

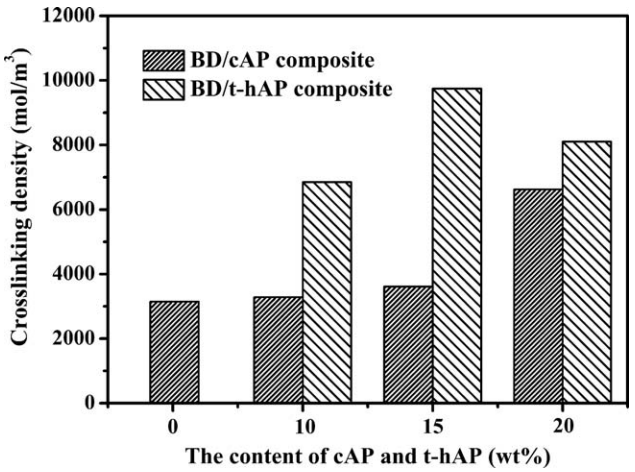

Figure 9. Crosslinking densities of BD resin, BD/cAP, and BD/t-hAP composites.

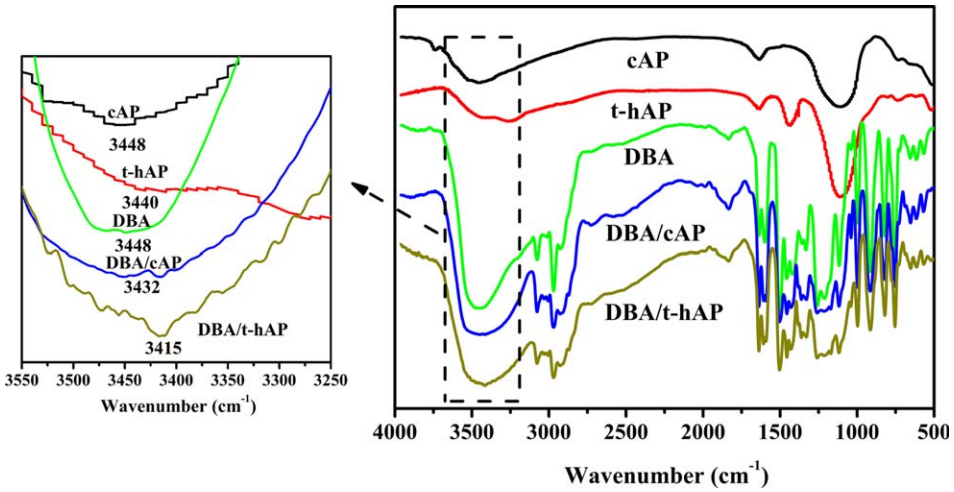

Figure 10. FTIR spectra of cAP, t-hAP, DBA/10cAP, and DBA/10t-hAP blends. [Color figure can be viewed in the online issue, which is available at wileyonlinelibrary.com.]

Flame Retarding Origin of BD/t-hAP Composites

The performance of a material is determined by its structure, so the structures should be studied first to answer the origin behind the difference in the flame retardance of BD resin, BD/cAP, and BD/t-hAP composites. For a thermosetting resin and related composites, their structure is divided into polymer chain and aggregation state structures. The former can be reflected by the curing mechanism, and the latter can be characterized by the crosslinking density.[57]

Since there are no reactive groups on the surfaces of cAP and t-hAP, so BD, BD/10cAP and BD/10t-hAP prepolymers have the same curing mechanism. Specifically, the curing mechanism of these samples contains multiple reactions, including "Ene addition" and "Diels-Alder" reactions between maleimide groups of BDM and allyl groups of DBA,[58] and the self-polymerization of BDM via double bond addition of maleimide groups.[59]

The crosslinking densities for BD resin, BD/cAP, and BD/t-hAP composites were estimated by the classical equation based on the statistical theory of rubber elasticity as shown in eq. (1):[60]

$$\rho_{(c)} = \frac{G'}{3\Phi RT} \quad (1)$$

where $\rho_{(c)}$ is crosslinking density; G' is the storage modulus of the composite in the rubbery plateau region from DMA tests, herein, G' is chosen as the modulus at the temperature (T) that is 20°C higher than glass transition temperature (T_g); Φ is the front factor, and assumed to be 1; R is the gas constant.

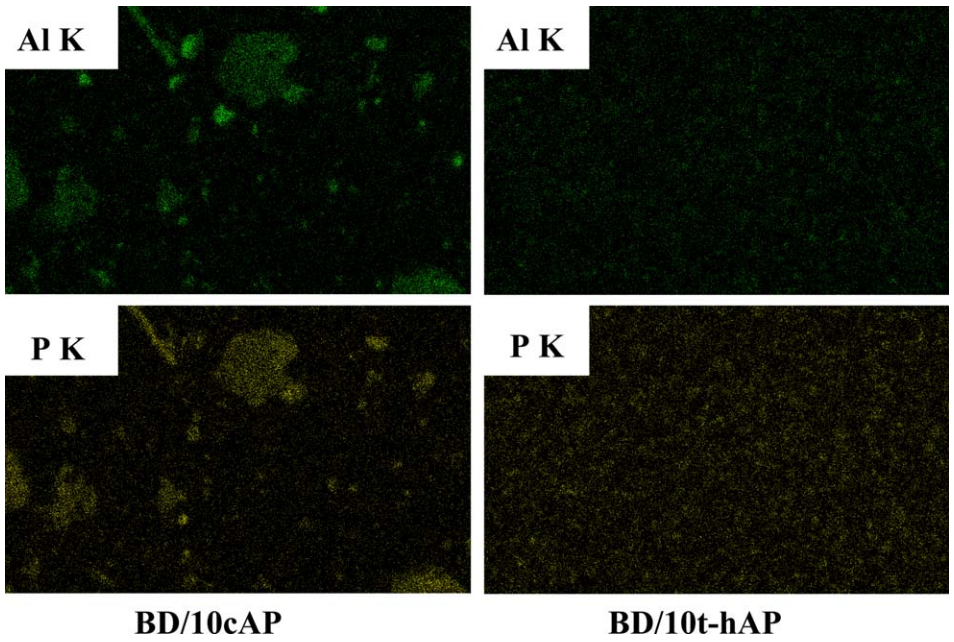

Figure 11. Al and P mappings of BD/10cAP and BD/10t-hAP composites. [Color figure can be viewed in the online issue, which is available at wileyonlinelibrary.com.]

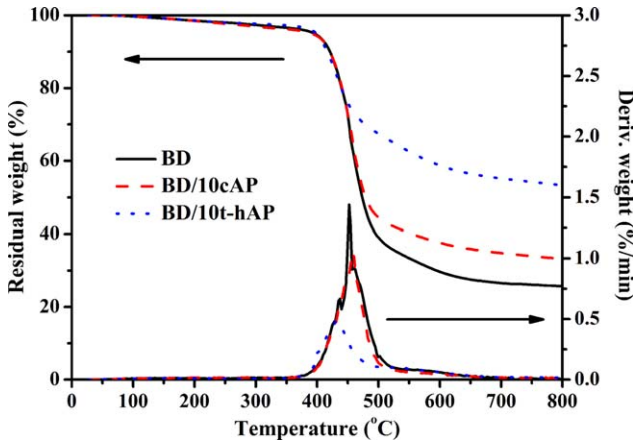

Figure 12. TG and DTG curves of BD resin, BD/10cAP, and BD/10t-hAP composites in a nitrogen atmosphere. [Color figure can be viewed in the online issue, which is available at wileyonlinelibrary.com.]

The corresponding $\rho_{(c)}$ values of BD resin, BD/cAP, and BD/t-hAP composites are depicted in Figure 9. The BD/t-hAP composite has higher crosslinking density than the BD/cAP composite with the same content of fillers. Since both surfaces of cAP and t-hAP have water molecules, so both fillers are expected to have interaction with DBA through hydrogen bonds. Figure 10 shows the FTIR spectra of DBA/10cAP and DBA/10t-hAP blends. The hydroxyl absorption (3448 cm^{-1}) is observed in the spectrum of either cAP, t-hAP, or DBA, which also appears in the spectra of two blends but shifts toward low wavenumber, suggesting that the spectra of these blends are not the simple combination of those of the components of the blends.[61] Meanwhile, the hydroxyl absorption (3415 cm^{-1}) in the spectrum of DBA/10t-hAP is lower and wider than that (3432 cm^{-1}) of DBA/10cAP, meaning that the hydrogen bond between t-hAP and DBA is stronger than that between cAP and DBA. It is mainly due to the fact that t-hAP has more —OH groups than cAP, providing more physical crosslinking points. As a result, BD/t-hAP composite has higher $\rho_{(c)}$ value than BD/cAP composite with the same loading of fillers.

To investigate the influence on the interaction between fillers on the morphological structure, the morphologies of two kinds of composites were observed. Figure 11 shows the Al and P mappings of composites using the EDS technique, the bright green and yellow dots represent Al and P atoms distributed in the BD resin, respectively. The aggregations are observed in either Al or P mapping of the BD/10cAP composite; however, this phenomenon doesn't appear in the BD/10t-hAP composite, clearly demonstrating that t-hAPs have better dispersion in BD resin while cAPs have not. The strong hydrogen bonds between t-hAP and DBA are responsible for this result.

The flame retardance of a polymer usually depends on many factors, among them the thermal stability, decomposition rate, producing rate of char and char yield during the degradation process are three key ones,[62] so it is worth paying great attentions on discussing the thermo degradation behavior. Figure 12 shows the TG and DTG curves of BD resin, BD/10cAP, and BD/10t-hAP composites in a nitrogen atmosphere. The addition of t-hAP or cAP only slightly increases the initial decomposition temperature (T_{di}), but greatly increases the Y_c at 800°C; specifically, the experimental Y_c value of BD/10t-hAP composite is 53.5%, which is much higher than the calculated value (31.8%) based on the "Mixture rule,"[63] while the experimental Y_c value (33.4%) of BD/10cAP composite is almost equal to that of calculated value (31.8%). so it is reasonable to state that t-hAP has high abilities of char-forming and retarding the thermal decomposition of BD resin, and this is beneficial to endow the crosslinked network with very good flame retardance.

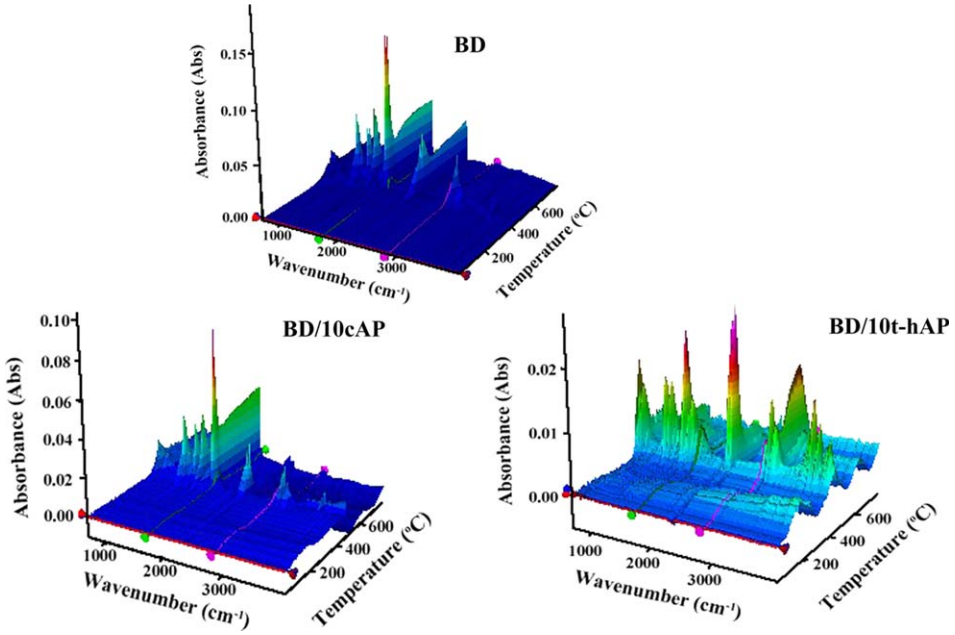

Figure 13. Three-dimensional FTIR spectra of BD resin, BD/10cAP, and BD/10t-hAP composites. [Color figure can be viewed in the online issue, which is available at wileyonlinelibrary.com.]

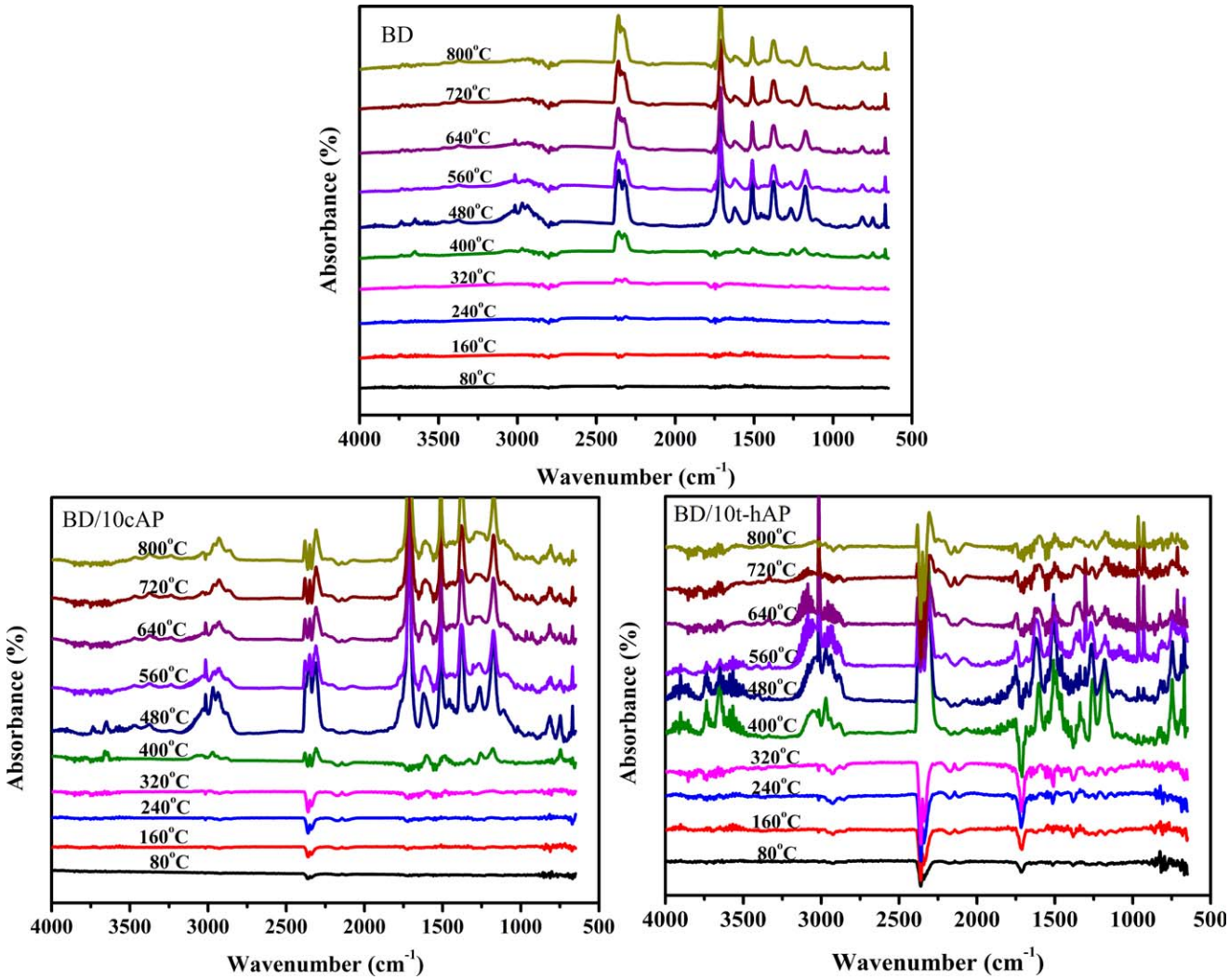

Figure 14. FTIR spectra of volatilized products at typical temperatures during the thermal degradation of BD resin, BD/10cAP, and BD/10t-hAP composites. [Color figure can be viewed in the online issue, which is available at wileyonlinelibrary.com.]

TG-IR technique is useful to reveal the thermal degradation mechanism of polymers by detecting the volatile degradation products.[64,65] Figure 13 shows the 3D TG-FTIR spectra of pyrolysis products of BD resin, BD/10cAP, and BD/10t-hAP composites. All spectra show the absorption peak (1715 cm^{-1}) assigning to carbonyl, and which is the strongest peak in the spectrum of either BD resin or BD/10cAP composite. With careful observation, it is found that the intensity of this peak is different in three spectra; the intensities of the absorption peak in the spectra of BD/10cAP and BD/10t-hAP composites are about 50% and 14% of that of BD resin, respectively, implying that the amount of the volatiles released from each composite is much less than that from BD resin. In other words, the presence of t-hAP or cAP can effectively retard the thermal decomposition of BD resin, especially t-hAP. This statement is further confirmed with following intensive discussion.

To provide an easier comparison, the FTIR spectra of the gaseous volatiles evolved at different temperatures corresponding to absorbance peaks are represented in Figure 14. When the temperature increases to 800°C, in the FTIR spectrum of BD resin, no stretching absorption of hydrocarbon ($CH/CH_2/CH_3$, 2800–3100 cm^{-1})[66] is observed, but the peak representing CO_2 stretching (2360 cm^{-1}) is still found, indicating that all organic compositions have been decomposed. With regard to the spectrum of BD/10cAP composite, in which there is a strong absorption assigning to hydrocarbon, while the absorption of CO_2 is weak, reflecting that some organic compounds remain and are stable. The obvious difference between BD resin and BD/10cAP composite demonstrates that the presence of cAP can effectively improve the thermal stability.

In the case of the FTIR spectrum of BD/10t-hAP composite, which is found to have other special characteristic that is totally different from those of BD resin and BD/10cAP composite. Specifically, the temperature for releasing pyrolysis products of BD/10t-hAP composite mainly ranges from 400 to 560°C, and few gases are produced when the temperature is higher than 640°C. Combined with above results from cone calorimeter tests, it is concluded that t-hAP is a good smoke suppressor. Besides, the

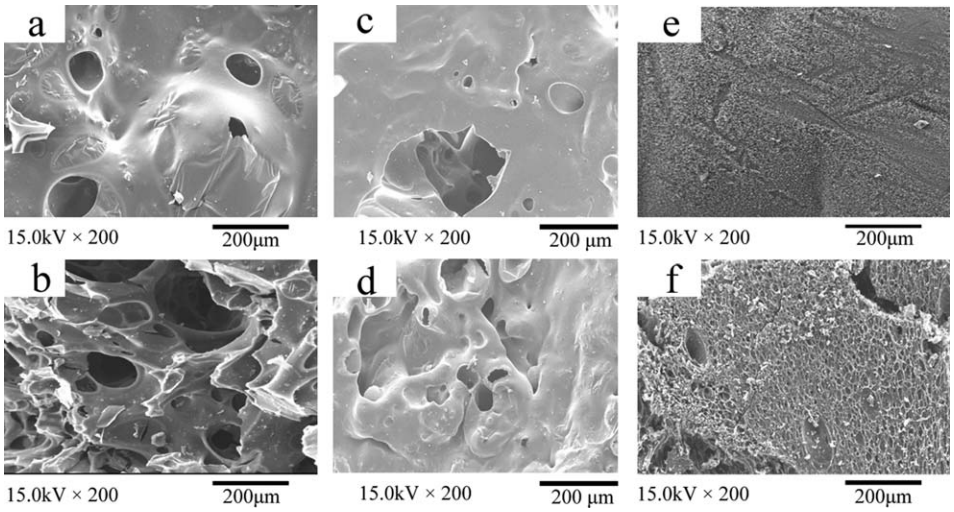

Figure 15. SEM micrographs of residual chars of BD resin (a, b), BD/10cAP composite (c, d) and BD/10t-hAP composite (e, f) after cone calorimeter tests.

evolved gas analysis of BD/10t-hAP composite exhibits the characteristic bands of H_2O (3500–3800 cm^{-1})[66] and NH_3 (3340, 970 cm^{-1}),[67] the H_2O and NH_4^+ could dilute the combustible gas, and thus helping to retard the combustion.

From above results, it is noted that the main evolved gas products for BD/10t-hAP composite are different from those of BD resin and BD/10cAP composite. The pyrolysis products of BD resin and BD/10cAP composite are mainly composed of CO_2 (2360 cm^{-1}), hydrocarbon (2800–3100 cm^{-1}) and compounds containing carbonyl (1715 cm^{-1}) that are responsible for the high HRR value as well as aromatic compounds (1512 cm^{-1}) that are the important source of smoke toxicity.[68] The BD/10t-hAP composite releases additional water and NH_3, and less production of gases after 640°C. It is known that the main flame retarding mechanism of $Mg(OH)_2$ and $Al(OH)_3$ is decomposing at a specific temperature with the elimination of water. This feature also appears in t-hAP, which is one important reason that t-hAP has outstanding flame retarding effect.

The residual char of a polymer can prevent the burning of combustible materials derived from the degradation and the entrance of heat; hence, the char plays an important role in the flame retarding performance.[69] Figure 15 shows the SEM micrographs of the residual chars of BD resin, BD/10cAP, and BD/10t-hAP composites after combustion tests. For the char of BD resin, both external and internal parts have large holes [Figure 15(a,b)]; this phenomenon is improved with the addition of cAP; however, some big holes are still observed in external and internal parts [Figure 15(c,d)]. A significantly different morphology appears in the char of BD/10cAP composite, the external part of BD/10t-hAP char is covered with a thick char layer [Figure 15(e)], and its internal part shows small, uniform and honeycomb porosity [Figure 15(f)]. Therefore, the addition of fillers and the nature of fillers play important roles on the morphology of chars, and t-hAP has an ability to form strong char layer.

CONCLUSIONS

Hexagonal aluminum phosphate ammonium taranakite (hAP) with uniform and small dimension was facilely synthesized using the homogeneous precipitation method. After treated at 150°C for 2 h, the resultant t-hAP has two crystal structures of aluminum phosphates. cAP and t-hAP have flame retarding effect, but t-hAP has much bigger effect due to its unique structure. Specifically, compared with cAP, the hexagonal structure and good dispersion of t-hAP in BD resin provide very effective heat insulating and barrier effects; furthermore, t-hAP has a bigger ability in forming strong char layer, and will release H_2O and NH_3 to dilute flammable gas. These multiple functions make t-hAP act as a super flame retardant.

ACKNOWLEDGMENTS

The authors thank the National Natural Science Foundation of China (21274104), the Priority Academic Program Development of Jiangsu Higher Education Institutions (PAPD), and Suzhou Applied Basic Research Program (SYG201141) for financially supporting this project.

REFERENCES

1. Wang, C. Q.; Ge, F. Y.; Sun, J.; Cai, Z. S. *J. Appl. Polym. Sci.* **2013**, *130*, 916.
2. Jung, N.; Kim, S. M.; Kang, D. H.; Chung, D. Y.; Kang, Y. S.; Chung, Y. H.; Choi, Y. W.; Pang, C.; Suh, K. Y.; Sung, Y. E. *Chem. Mater.* **2013**, *25*, 1526.
3. Song, P. A.; Shen, Y.; Du, B. X.; Guo, Z. H.; Fang, Z. P. *Nanoscale* **2009**, *1*, 118.
4. Ma, H. Y.; Wang, J.; Fang, Z. P. *Polym. Degrad. Stab.* **2012**, *97*, 1596.
5. Duquesne, S.; Fontaine, G.; Cerin-Delaval, O.; Gardelle, B.; Tricot, G.; Bourbigot, S; *Thermochim. Acta* **2013**, *551*, 175.
6. Wang, X.; Hu, Y.; Song, L.; Xing, W. Y.; Lu, H. D. *J. Polym. Sci. Pol. Phys.* **2010**, *48*, 693.

7. Hapuarachchi, T. D.; Peijs, T. *Compos. Part A: Appl. S.* **2010**, *41*, 954.
8. Brehme, S.; Schartel, B.; Goebbels, J.; Fischer, O.; Pospiech, D.; Bykov, Y.; Doring, M. *Polym. Degrad. Stab.* **2011**, *96*, 875.
9. Schartel, B.; Weiss, A.; Sturm, H.; Kleemeier, M.; Hartwig, A.; Vogt, C.; Fischer, R. X. *Polym. Adv. Technol.* **2011**, *22*, 1581.
10. Konnicke, D.; Kuhn, A.; Mahrholz, T.; Sinapius, M. *J. Mater. Sci.* **2011**, *46*, 7046.
11. Xu, T.; Huang, X. M. *J. Anal. Appl. Pyrol.* **2010**, *87*, 217.
12. Antunes, M.; Velasco, J. I.; Haurie, L. *J. Cell. Plast.* **2013**, *47*, 17.
13. Wang, Z. Y.; Liu, Y.; Wang, Q. *Polym. Degrad. Stab.* **2010**, *95*, 945.
14. Wang, Z. Z.; Qu, B. J.; Fan, W. C.; Huang, P. *J. Appl. Polym. Sci.* **2001**, *81*, 206.
15. Chung, D. D. L. *J. Mater. Sci.* **2003**, *38*, 2785.
16. Hoshii, S.; Kojima, A.; Tamaki, T.; Otani, S. *J. Mater. Sci. Lett.* **2000**, *19*, 557.
17. Han, H. J.; Kim, D. P. *J. Sol-Gel Sci. Technol.* **2003**, *26*, 223.
18. Lu, Z. Y.; Geng, H. R.; Zhang, M. X.; Hou, X. Q. *Chinese. Sci. Bull.* **2008**, *53*, 3073.
19. Wang, K. T.; Cao, L. Y.; Huang, J. F.; Fei, J.; Zhang, B. Y. *Ceram. Int.* **2013**, *39*, 1037.
20. Tricot, G.; Nicolaus, N.; Diss, P.; Montagne, L. *Carbon* **2012**, *50*, 3440.
21. Knohl, S.; Roy, A. K.; Lungwitz, R.; Spanle, S.; Mkler, T.; Nestler, D. J.; Wielage, B.; Schulze, S.; Hietschold, M.; Wulff, H.; Heim, C. A.; Seide, F.; Zahn, D. R. T.; Goedelt, W. A. *ACS Appl. Mater. Interfaces* **2013**, *5*, 6161.
22. Deng, S. F.; Wang, C. F.; Zhou, Y.; Huang, F. R.; Du, L. *Int. J. Appl. Ceram. Tec.* **2011**, *8*, 360.
23. Deng, S. F.; Wang, C. F.; Zhou, Y.; Huang, F. R.; Du, L. *Mater. Sci. Eng. A* **2008**, *477*, 96.
24. Sun, Z. Q.; Gu, A. J.; Liang, G. Z.; Dai, S. K.; Yuan, L. *J. Appl. Polym. Sci.* **2009**, *113*, 3427.
25. Gu, A. J.; Liang, G. Z. *Polym. Degrad. Stab.* **2003**, *80*, 383.
26. Mariappan, T.; You, Z.; Hao, J. W.; Wilkie, C. A. *Eur. Polym. J.* **2013**, *49*, 3171.
27. Lavorgna, M.; Romeo, V.; Martone, A.; Zarrelli, M.; Giordano, M.; Buonocore, G. G.; Qu, M. Z.; Fei, G. X.; Xia, H. S. *Eur. Polym. J.* **2013**, *49*, 428.
28. Yuan, B. H.; Bao, C. L.; Guo, Y. Q.; Song, L.; Liew, K. M.; Hu, Y. *Ind. Eng. Chem. Res.* **2012**, *51*, 14065.
29. Liu, X. Q.; Liu, J. Y.; Cai, S. *J. Polym. Compos.* **2012**, *33*, 918.
30. Wang, L.; Sanchez-Soto, M.; Maspoch, M. L. *Mater. Des.* **2013**, *52*, 609.
31. Xing, W. Y.; Jie, G. X.; Song, L.; Wang, X.; Lv, X. Q.; Hu, Y. A. *Mater. Chem. Phys.* **2011**, *125*, 196.
32. Lv, J. P.; Qiu, L. Z.; Qu, B. J. *Nanotechnology* **2004**, *15*, 1576.
33. Yao, W.; Gu, A. J.; Liang, G. Z.; Zhuo, D. X.; Yuan, L. *Polym. Adv. Technol.* **2012**, *23*, 326.
34. Kawamura, K.; Shibuya, K.; Okuwaki, A. *Mater. Res. Bull.* **2007**, *42*, 256.
35. Wei, L. Q.; Ye, S. F.; Tian, Y. J.; Xie, Y. S.; Chen, Y. F. J. *Cryst. Growth* **2009**, *311*, 3359.
36. Chen, C. M.; Jehng, J. M. *Catal. Lett.* **2003**, *85*, 73.
37. Bleam, W. F.; Pfeffer, P. E.; Frye, J. S. *Phys. Chem. Miner.* **1989**, *16*, 809.
38. Schwieger, W.; Altenschildesche, H. M. Z.; Kokotailo, G. T.; Fyfe, C. A. Z. *Anorg. Allg. Chem.* **1998**, *624*, 1712.
39. Neira, I. S.; Kolen'ko, Y. V.; Lebedev, O. I.; Van Tendeloo, G.; Gupta, H. S.; Guitian, F.; Yoshimura, M. *Cryst. Growth. Des.* **2009**, *9*, 466.
40. Pluth, J. J.; Smith, J. V. *Acta Cryst.* **1984**, *C40*, 2008.
41. Chen, Y. H.; Liu, Y.; Wang, Q.; Yin, H.; Kierkels, N. *Polym. Degrad. Stab.* **2003**, *81*, 215.
42. Cogen, J. M.; Lin, T. S.; Lyon, R. E. *Fire Mater.* **2009**, *33*, 33.
43. Schartel, B.; Hull, T. *Fire Mater.* **2007**, *31*, 327.
44. Lu, H. D.; Wilkie, C. A.; Ding, M.; Song, L. *Polym. Degrad. Stab.* **2011**, *96*, 1219.
45. Song, P. A.; Zhao, L. P.; Cao, Z. H.; Fang, Z. P. *J. Mater. Chem.* **2011**, *21*, 7282.
46. Tai, Q. L.; Shan, X. Y.; Song, L.; Lo, S. M.; Yuen, R. K. K.; Hu, Y. *Polym. Compos.* **2014**, *35*, 167.
47. Chang, S. Q.; Xie, T. X.; Yang G. S. *Polym. Degrad. Stab.* **2006**, *91*, 3266.
48. Jiao, C. M.; Chen, X. L. *J. App. Polym. Sci.* **2010**, *116*, 1889.
49. Lorenzetti, A.; Modesti, M.; Besco, S.; Hrelja, D.; Donadi, S. *Polym. Degrad. Stab.* **2011**, *96*, 1455.
50. Hull, T. R.; Stec, A. A.; Lebek, K.; Price, D. *Polym. Degrad. Stab.* **2007**, *92*, 2239.
51. Hull, T. R.; Quinn, R. E.; Areri, I. G.; Purser, D. A. *Polym. Degrad. Stab.* **2002**, *77*, 235.
52. Gallo, E.; Braun, U.; Schartel, B.; Russo, P.; Acierno, D. *Polym. Degrad. Stab.* **2007**, *94*, 1245.
53. Sheng, F. F.; Tang, X. Z.; Zhang, S.; Ding, X. J.; Yu, Z. Z.; Qiu, Z. B. *Polym. Adv. Technol.* **2012**, *23*, 137.
54. Qu, H. Q.; Liu, C. H.; Wu, W. H.; Chen, L. Z.; Xu, J. Z. *J. Therm. Anal. Calorim.* **2014**, *115*, 1081.
55. Kim, S. *J. Polym. Sci. Part B-Polym. Phys.* **2003**, *41*, 936.
56. Yen, Y. Y.; Wang, H. T.; Guo, W. *J. Polym. Degrad. Stab.* **2012**, *97*, 863.
57. Zhuo, D. X.; Gu, A. J.; Liang, G. Z.; Hu, J. T.; Yuan, L.; Chen, X. X. *J. Mater. Sci.* **2011**, *46*, 1571.
58. Zhuo, D. X.; Gu, A. J.; Liang, G. Z.; Hu, J. T.; Yuan, L.; Chen, X. X. *J. Mater. Chem.* **2011**, *21*, 6584.
59. Xiong, Y.; Boey, F. Y. C.; Rath, S. K. *J. Appl. Polym. Sci.* **2003**, *90*, 2229.
60. Rozenberg, B. A.; Dzhavadyan, E. A.; Morgan, R.; Shin, E. *Polym. Adv. Technol.* **2002**, *13*, 837.
61. Kumar, S.; Nair, R. C. P.; Ninan, K. N. *Eur. Polym. J.* **2009**, *45*, 494.
62. Chen, Y. H.; Liu, Y.; Wang, Q.; Yin, H.; Kierkels, N. *Polym. Degrad. Stab.* **2003**, *81*, 215.
63. Mi, Y. N.; Liang, G. Z.; Gu, A. J.; Zhao, F. P.; Yuan, L. *Ind. Eng. Chem. Res.* **2013**, *52*, 3342.

64. Wu, K.; Song, L.; Hu, Y.; Lu, H. D.; Kandolac, B. K.; Kandare, E. *Prog. Org. Coat.* **2009**, *65*, 490.

65. Zhang, P.; Hu, Y.; Song, L.; Ni, J. X.; Xing, W. Y.; Wang, J. *Sol. Energy Mater. Sol. Cells* **2010**, *94*, 360.

66. Wu, K.; Zhang, Y. K.; Zhang, K.; Shen, M. M.; Hu, Y. *J. Anal. Appl. Pyrol.* **2012**, *94*, 196.

67. Tai, Q. L.; Yuen, R. K. K.; Yang, W.; Qiao, Z. H.; Song, L.; Hu, Y. *Compos. Part A-Appl. Sci. Manuf.* **2012**, *43*, 415.

68. Xu, T.; Huang, X. M. *J. Anal. Appl. Pyrol.* **2010**, *87*, 217.

69. Chen, J.; Liu, S. M.; Zhao, J. Q. *Polym. Degrad. Stab.* **2011**, *96*, 1508.